13th International Symposium on Particle Image Velocimetry – ISPIV 2019
Munich, Germany, July 22-24, 2019

Data assimilation-based flow field reconstruction from particle tracks over multiple time steps

Young Jin Jeon[1]*, Markus Müller[1], Dirk Michaelis[1], Bernhard Wieneke[1]

[1]LaVision GmbH, Göttingen, Germany

*yjeon@lavision.de

Abstract

The present work reports on how to deal with particle track information over multiple time steps so to expect an improvement on the data assimilation methods such as the Vortex-in-Cell plus (VIC+) method and the FlowFit method, which reconstruct a flow field on a Cartesian grid from particle tracks. Considering the number of realizations from PTV measurement and the degree of freedom (DOF) of a target flow field to be reconstructed, there are two possible ways: increasing realizations and decreasing DOF. Among those, the former, increasing realizations, is only dealt with in this study and is achieved by adding information projected from particle tracks at neighboring time steps. VIC# is chosen as a data assimilation-based method, which supplements additional constraints and coarse-grid approximation to the VIC+ method. The present method is applied to a time-resolved STB measurement for water jet from a circular nozzle. Clearer evolution of flow structures is observed while the increment of the computation time due to the increased realizations is neglected.

1 Introduction

Shake-the-Box (STB, Schanz et al. 2013, 2016) method has emerged as a 4D particle tracking velocimetry (4D PTV) technique since it is capable of reconstructing ghostless Lagrangian tracks from densely seeded particle images using advanced iterative particle reconstruction (IPR, Wieneke 2013). IPR allows STB to work for very dense particle volumes, which cannot be dealt with by conventional PTV methods and, therefore, often inevitably require tomographic reconstruction (Elsinga et al. 2006, Novara et al. 2010, Lynch and Scarano 2015). A set of particle tracks in volume, however, require intermediate processing, which converts the scattered information to a regular vector field on a Cartesian grid, for further data-processing and visualizations. The intermediate processing has three possible methodologies: using unstructured grid based on Voronoi tessellation and Delaunay triangulation (Neeteson and Rival 2015), the adaptive Gaussian windowing (AGW, Agüí and Jiménez 1987) which gathers scattered information with weighting, and data assimilation which optimizes a flow field by considering governing equations. As data assimilation-based methods, the VIC+ (Schneiders and Scarano 2016) and the FlowFit (Gesemann 2015, Gesemann et al. 2016) have shown significant improvements in spatial resolution and reconstruction fidelity regardless of imbalanced local particle concentration. Recently, VIC+ is supplemented with additional constraints and coarse-grid approximation in order both to suppress computational residuals near the computational boundary and to reduce computation time (VIC#, Jeon et al. 2018).

Even though STB provides time-resolved particle tracks, the data assimilation-based methods generally deal with filtered information at a specific interrogation time step. Time-resolved Lagrangian particle tracks, however, are capable of providing more information than what the

current methods utilize. The additional information yields an increased ratio of the number of realizations from STB measurement to the degree of freedom (DOF) of the reconstruction target. This increment can be achieved in two ways. The simplest way is that information at neighboring time steps is projected onto the interrogation time step using the Taylor hypothesis while keeping its position, which differs from the position at the interrogation time step. The projection can thus increase the number of realization while preserving the DOF. It means that there is no significant increment in computation time. Another way is an optimization of multiple time steps at once. Although this way requires more computation time, time derivatives are subordinated to the time-resolved flow fields. As a pilot approach, the first way in cooperated with VIC# is only considered in this study. Figure 1 illustrates how information is transferred from an STB measurement to the assimilation methods.

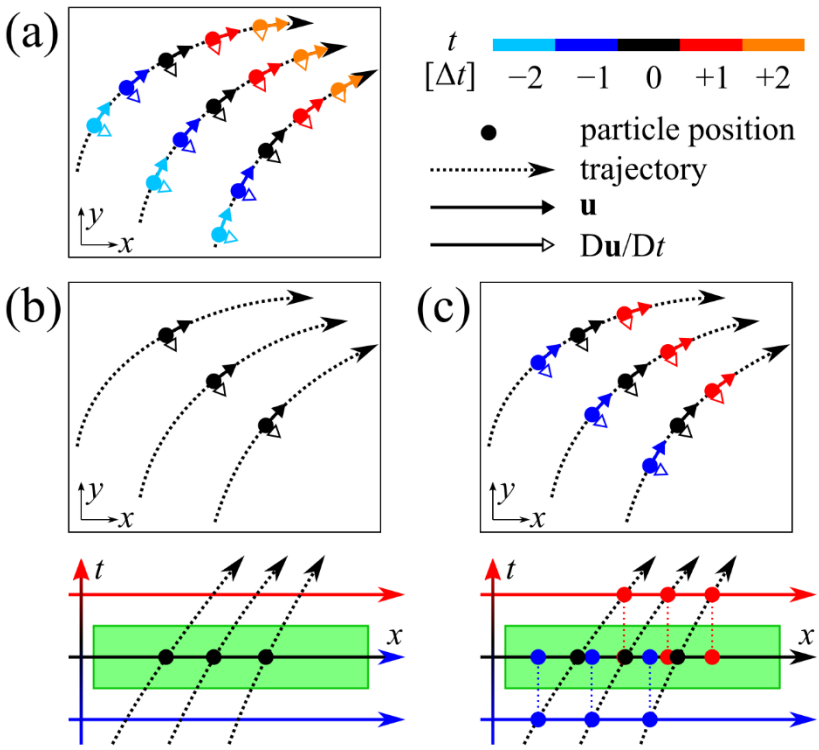

Figure 1: Illustration of data transfer from STB measurement to data assimilation methods: (a) STB measurement, (b) reconstruction of a single time step, e.g., VIC+, FlowFit, and VIC#, (c) reconstruction of a single time step at $t = t_0$ using projected vectors from neighboring time steps, $t = t_0 \pm 1\Delta t$. The *green boxes* indicate the domain to be reconstructed at once.

2 Description of method

Input data for the data assimilation method, e.g., VIC+, VIC#, and FlowFit, is a set of scattered particle information which consists of position ($\mathbf{x}$), velocity ($\mathbf{u}$), and material acceleration ($\mathrm{D}\mathbf{u}/\mathrm{D}t$):

$$\mathbf{f}_{\mathrm{STB}}(t) = \left\{\left(\mathbf{x}, \mathbf{u}, \frac{\mathrm{D}\mathbf{u}}{\mathrm{D}t}\right)_1, \ldots, \left(\mathbf{x}, \mathbf{u}, \frac{\mathrm{D}\mathbf{u}}{\mathrm{D}t}\right)_N\right\}, \tag{1}$$

where N is the number of particle tracks. The data assimilation methods iteratively optimize a flow field on a Cartesian grid while minimizing the cost function:

$$J = J_{\mathbf{u}} + \alpha^2 J_{\mathrm{D}\mathbf{u}/\mathrm{D}t} + J_{\mathrm{etc.}}, \tag{2}$$

where $J_{\mathbf{u}}$ and $J_{\mathrm{D}\mathbf{u}/\mathrm{D}t}$ indicates sums of disparities between the STB measurement and the reconstructed flow field:

$$J_{\mathbf{u}} = \sum_{n=1}^{N} \left\| \mathbf{u}_n - \mathbf{u}_{\mathrm{STB},n} \right\|^2 \tag{3a}$$

$$J_{\mathrm{D}\mathbf{u}/\mathrm{D}t} = \sum_{n=1}^{N} \left\| \left. \frac{\mathrm{D}\mathbf{u}}{\mathrm{D}t} \right|_n - \left. \frac{\mathrm{D}\mathbf{u}}{\mathrm{D}t} \right|_{\mathrm{STB},n} \right\|^2. \tag{3b}$$

And $J_{\mathrm{etc.}}$ denotes the additional cost function of VIC#. Here the vectors fractional to the Cartesian grid, $\mathbf{u}_n$ and $\mathrm{D}\mathbf{u}/\mathrm{D}t|_n$, are interpolated from the reconstructed flow field. Note that the FlowFit is able to evaluate the fractional vectors using B-splines.

In addition to the reference input data, $\mathbf{f}_{\mathrm{STB}}(t_0)$, the present method considers more information from neighboring time steps, i.e., $\mathbf{f}_{\mathrm{STB}}(t_0 + m\Delta t)$ where $m = -M, \ldots, -1, 1, \ldots, M$. The velocity vector and material acceleration vector at $(t_0 + m\Delta t)$ can be expressed using the reconstructed flow field at t_0 based on the first order Taylor expansion:

$$\mathbf{u}_{\mathrm{STB}}(t_0 + m\Delta t) \cong \mathbf{u}(t_0) + m\Delta t \frac{\partial \mathbf{u}}{\partial t}(t_0) \tag{4a}$$

$$\left. \frac{\mathrm{D}\mathbf{u}}{\mathrm{D}t} \right|_{\mathrm{STB}} (t_0 + m\Delta t) \cong \frac{\mathrm{D}\mathbf{u}}{\mathrm{D}t}(t_0) + m\Delta t \frac{\partial}{\partial t}\left(\frac{\mathrm{D}\mathbf{u}}{\mathrm{D}t}(t_0) \right) \tag{4b}$$

Note that all vectors are defined at the same location, $\mathbf{x}$ $(t_0 + m\Delta t)$. Here the time derivative of material acceleration, which is not generally obtained, can be calculated after neglecting the second time derivative term and thus expressed in a tensor notation:

$$\frac{d}{dt}\left(\frac{\mathrm{D}u_i}{\mathrm{D}t} \right) = \frac{\partial^2 u_i}{\partial t^2} + \frac{\partial}{\partial t}\left(\mathrm{u}_j \frac{\partial u_i}{\partial x_j} \right) \cong \frac{\partial \mathrm{u}_j}{\partial t} \frac{\partial u_i}{\partial x_j} + \mathrm{u}_j \frac{\partial}{\partial x_j}\left(\frac{\partial \mathrm{u}_j}{\partial t} \right). \tag{5}$$

Assuming that the second terms are interpolated from the lately reconstructed flow field, the first terms in the right-hand side of Eqs. (4a) and (4b) can be regarded as the projected vectors:

$$\mathbf{u}(t, m)_{\mathrm{Proj.}} \cong \mathbf{u}_{\mathrm{STB}}(t + m\Delta t) - m\Delta t \frac{\partial \mathbf{u}}{\partial t}(t) \tag{6a}$$

$$\frac{\mathrm{D}\mathbf{u}}{\mathrm{D}t}(t, m)_{\mathrm{Proj.}} \cong \left. \frac{\mathrm{D}\mathbf{u}}{\mathrm{D}t} \right|_{\mathrm{STB}} (t + m\Delta t) - m\Delta t \frac{\partial}{\partial t}\left(\frac{\mathrm{D}\mathbf{u}}{\mathrm{D}t}(t) \right). \tag{6b}$$

Note that the time derivative terms should be thus updated at each iteration. The additional information from the neighboring time steps can be then considered in the optimization as a modified sum of disparities:

$$J'_{\mathbf{u}} = \sum_{m=-M}^{+M} \sum_{n=1}^{N} \left\| \mathbf{u}(t + m\Delta t)_{\mathrm{Proj.},n} - \mathbf{u}(t, m)_{\mathrm{STB},n} \right\|^2 \tag{7a}$$

$$J'_{\mathrm{D}\mathbf{u}/\mathrm{D}t} = \sum_{m=-M}^{+M} \sum_{n=1}^{N} \left\| \frac{\mathrm{D}\mathbf{u}}{\mathrm{D}t}(t + m\Delta t)_{\mathrm{Proj.},n} - \frac{\mathrm{D}\mathbf{u}}{\mathrm{D}t}(t, m)_{\mathrm{STB},n} \right\|^2. \tag{7b}$$

When $m = 0$, the projected vectors are identical to the STB vectors, e.g., $\mathbf{u}\ (t, 0)_{\mathrm{Proj.}} \equiv \mathbf{u}\ (t)_{\mathrm{STB}}$.

As a result, the number of realizations is increased $(2M + 1)$ times. Considering that the filtered vectors at consecutive time steps along each trajectory are strongly coherent to each other, the increment would be less valid than $(2M + 1)$. However, since the filtering procedure evaluates vectors from raw particle positions of STB data using least-square-based fitting with a specific filtering range in time-space, it can be regarded that the filtered vectors at consecutive time steps contain diversity for flow characteristics. Therefore, one can expect that the increased number of realizations strengthen not only the reconstruction quality but also the temporal coherence of vortical structures.

3 Results

Images from the measurement of a circular jet in water (Violato and Scarano, 2011) are processed using STB. The nozzle exit diameter is 10 mm, and the exit velocity of the jet is 0.5 m/s. Polyamide particles are seeded with a concentration of 0.031 ppp and illuminated by a Quantronix *Darwin-Duo* Nd-YLF laser. Four LaVision *HighSpeedStar 6* CMOS cameras operate in 1.3 kHz to obtain a series of time-resolved images. The measurement domain for STB analysis has a dimension of 50 × 70 × 50 mm^3. Particle positions, velocity, and material acceleration are obtained from the second-order polynomial trajectory model with a filter length L. A computation domain of 28 × 56 × 28 mm^3 is discretized with a grid spacing of h = 0.47 mm (7 voxels), and thus 61 × 121 × 61 grid points are considered in the VIC# reconstruction. Flow fields on two coarse grid schemes with h_2 = 28 voxels and h_1 = 14 voxels are precedently reconstructed after 200 iterations each and provide an initial condition for the final grid scheme. 100 iterations are conducted for the final grid scheme. All the analysis, i.e., STB, VIC#, and the present method, are conducted using DaVis 10 software. Figure 2 demonstrates the results of STB and VIC#, respectively.

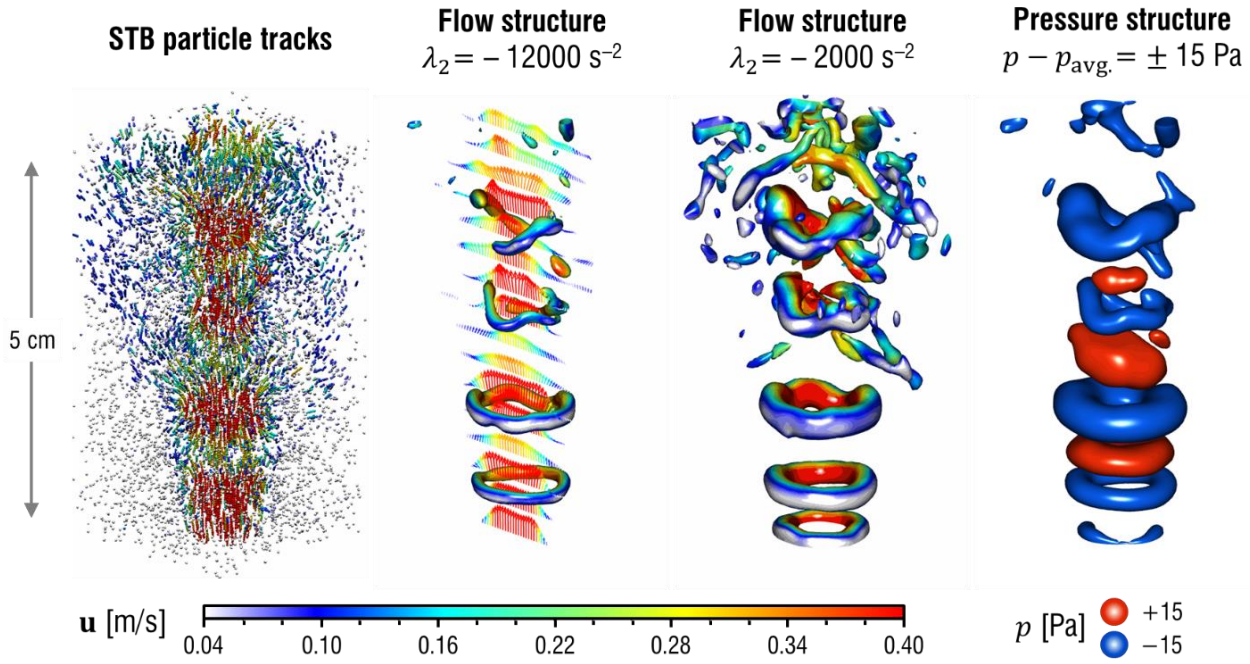

Figure 2: Results of STB and VIC# analyses. For VIC#, a filter length of $L = 9\Delta t$ is used.

	Reference ($M = 0$)	**Present** ($M = (L/\Delta t - 1)/2$)
$L = 5\Delta t$	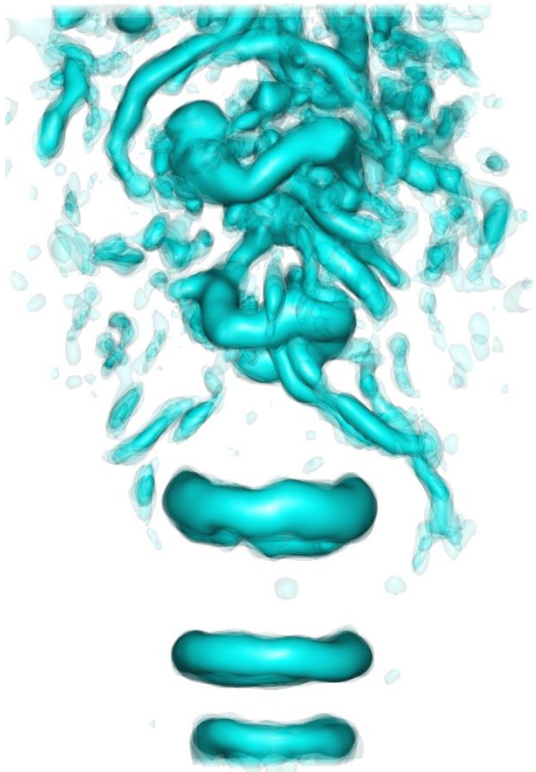	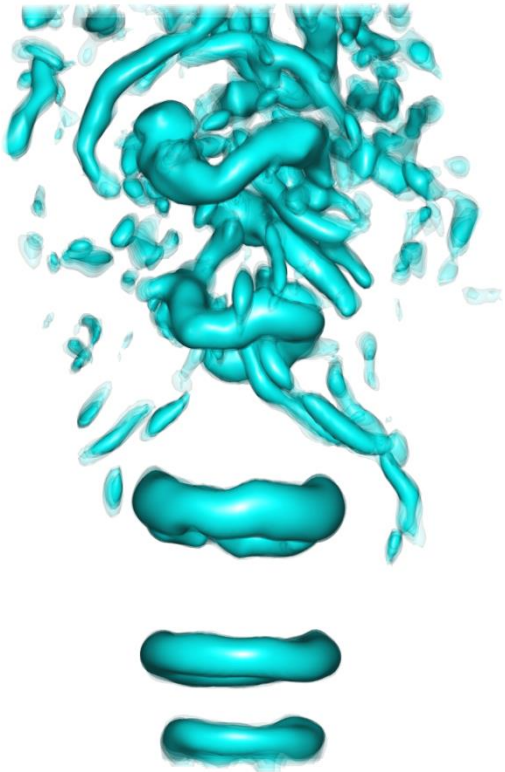
$L = 9\Delta t$	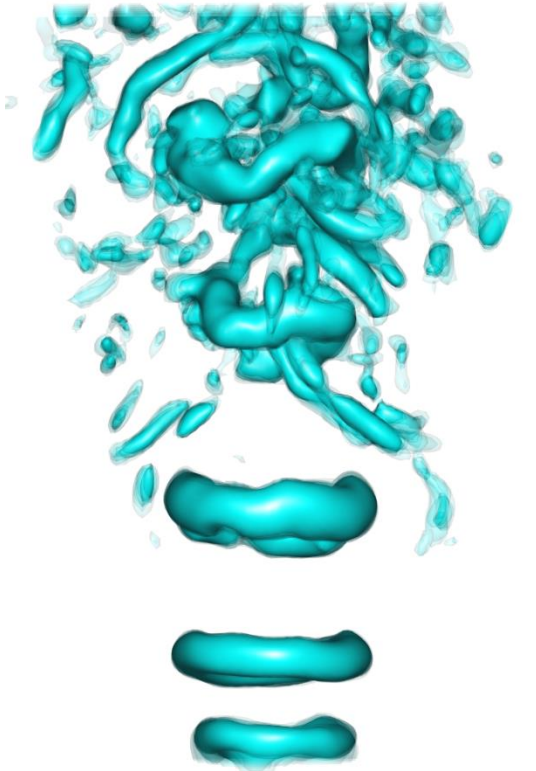	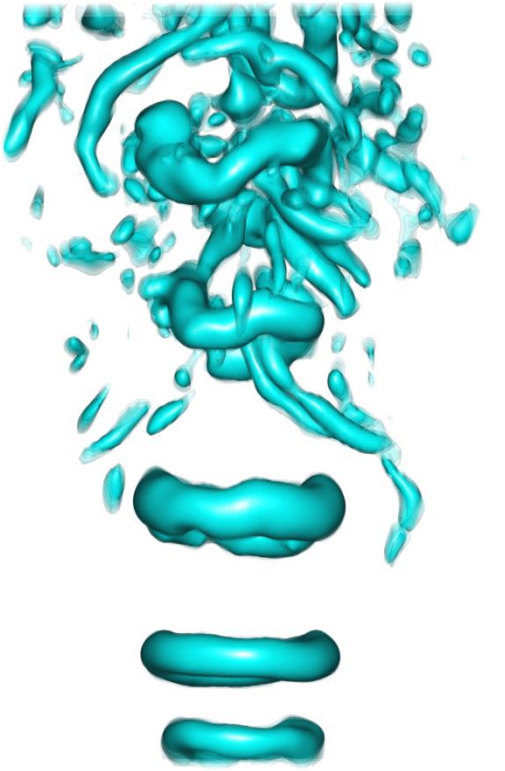

Figure 3: Superimposed iso-surface images of swirling strength, $\lambda = -2500$ s^{-2}. The images from 8 time steps are shifted downward proportional to the respective elapsed time, i.e., $-\mathbf{v}_C\,(t - t_0)$.

The high random noises in the particle images due to the time-resolved experimental apparatuses are directly reflected in the particle track information, i.e., position, velocity, and material acceleration. Therefore, a large denoising factor (f_{DN} = 5.0) is chosen for the VIC# and the present method. Here, the denoising factor emphasizes correction of velocity field based on the pressure field, and thus noisy vortical structures smaller than pressure structures are smoothed out. Two filter lengths, $L = 5\Delta t$ and $9\Delta t$, are selected for the modeling of trajectory based on second-order polynomial function. For the present method, all the trajectory information is projected onto the interrogation time step, i.e., M = 2 and 4, respectively. The computation parameters for the four cases are detailed in Table 1.

	Reference $5\Delta t$	Reference $9\Delta t$	Present $5\Delta t$	Present $9\Delta t$
L	$5\Delta t$	$9\Delta t$	$5\Delta t$	$9\Delta t$
M	0	0	2	4

Table 1: Comparison of the test cases. The reference cases and the present cases correspond to Fig. 1(b) and Fig. 1(c), respectively.

Figure 3 visualizes how well the flow structures are preserved during their convective movement. Images, which represent iso-surface of swirling strength, from 8 consecutive time steps are superimposed each other with different transparencies to have the same resulting image intensity. The images are displaced proportionally to the time elapsed from the first image. This convection velocity in the vertical direction, $\mathbf{v}_C$ = 0.18 m/s, is estimated from the movement of the vortex ring generated and driven by the core jet. Figure 4 zooms in on two partial structures, the second vortex ring from the nozzle and the fifth one, which is distorted, in Fig. 3.

	Reference (M = 0)	**Present** ($M = (L/\Delta t - 1)/2$)
$L = 5\Delta t$	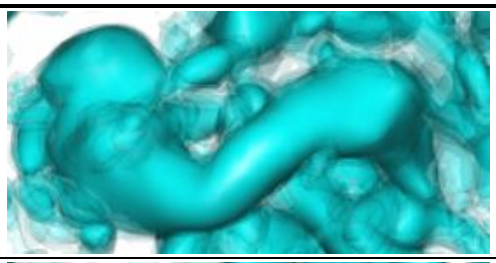	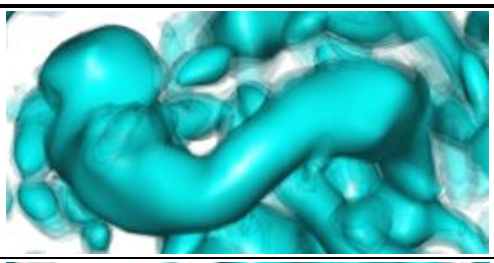
$L = 9\Delta t$	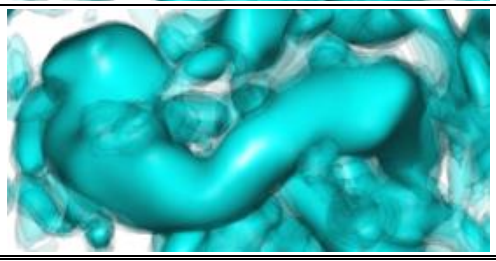	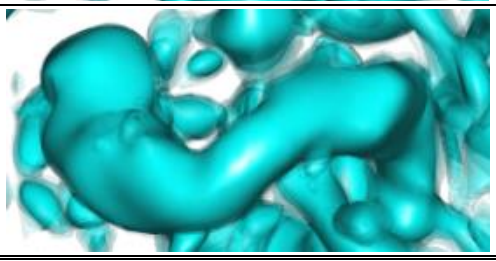
$L = 5\Delta t$		
$L = 9\Delta t$		

Figure 4: Partially zoomed images of Fig. 3.

It is visible that the present method improves the coherency of flow structures in time-space. Even though the present method reconstructs a flow field at each time step individually, all the major structures are consistently observed. The structures distant from the core look like afterimages due to the relatively slower convection velocity. Considering two cases, Reference 9Δt and Present 5Δt, which employ the same particle track information from t = -4Δt to t = +4Δt, the present method shows more consistent flow structures. It implies that the enhancement of dynamic range by increasing L in the least-square fitting is less effective than by increasing the number of realizations in the present method. In this study, the number of projected time steps, 2M, is selected as the maximum, ($L/\Delta t$ – 1). However, it should be restricted by how strong the second derivative term locally is. It means that an optimal temporal separation similar to that proposed Sciacchitano et al. (2012) would be considered in a further study.

4 Conclusion

This study has investigated a way to improve the data assimilation method by adding more information from different time steps. Particle track information at neighboring time steps is projected onto the interrogation time step based on the Taylor hypothesis. Since the information density of input data is increased, reconstructed flow structures have more temporal coherency with the consecutive time steps. This projecting method only leads to little computational overheads. Even though the present study only deals with the VIC# method, the same principle is applicable to the other data assimilation methods such as the VIC+ and the FlowFit.

References

Agüí JC and Jiménez J (1987) On the performance of particle tracking. *Journal of fluid mechanics* 185:447–468

Elsinga GE, Scarano F, Wieneke B, and van Oudheusden BW (2006) Tomographic particle image velocimetry. *Experiments in fluids* 41:933-947

Gesemann S (2015) From particle tracks to velocity and acceleration fields using B-splines and penalties. *arXiv* 1510.09034

Gesemann S, Huhn F, Schanz D, and Schröder A (2016) From noisy particle tracks to velocity, acceleration and pressure fields using B-splines and penalties. In *18th international symposium on applications of laser and imaging techniques to fluid mechanics, Lisbon, Portugal, July 4–7*

Jeon YJ, Schneiders JFG, Müller M, Michaelis D, and Wieneke B (2018) 4D flow field reconstruction from particle tracks by VIC+ with additional constraints and multigrid approximation. In *Proceedings 18th International Symposium on Flow Visualization. ETH Zurich. June 26–29*

Lynch KP and Scarano F (2015) An efficient and accurate approach to MTE-MART for time-resolved tomographic PIV. *Experiments in Fluids* 55:66

Neeteson NJ and Rival DE (2015) Pressure-field extraction on unstructured flow data using a Voronoi tessellation-based networking algorithm: a proof-of-principle study. *Experiments in Fluids* 56:44

Novara M, Batenburg KJ, and Scarano F (2010) Motion tracking-enhanced MART for tomographic PIV. *Measurement Science and Technology* 21:035401

Schanz D, Schröder A, Gesemann S, Michaelis D, and Wieneke B (2013) Shake The Box: A highly efficient and accurate tomographic particle tracking velocimetry method using prediction of particle positions, In *10th Int. Symp. on particle image velocimetry – PIV13, Delft, The Netherlands, July 1–3*

Schanz D, Gesemann S, and Schröder A (2016) Shake-The-Box: Lagrangian particle tracking at high particle image densities. *Experiments in Fluids* 57:70

Schneiders JFG and Scarano F (2016) Dense velocity reconstruction from tomographic PTV with material derivatives. *Experiments in Fluids* 57:139

Sciacchitano A, Scarano F, and Wieneke B (2012) Multi-frame pyramid correlation for time-resolved PIV. *Experiments in Fluids* 53:1087–1105

Violato D and Scarano F (2011) Three-dimensional evolution of flow structures in transitional circular and chevron jets. *Phys Fluids* 23:124104

Wieneke B (2012) Iterative reconstruction of volumetric particle distribution. *Measurement Science and Technology* 24:024008